

AD-A143 231

TURBULENT DIFFUSION DISSIPATION AND WINDS FROM
CALIBRATED PHOTOGRAPHS OF (U) PHOTOMETRICS INC WOBURN
MA C A TROWBRIDGE 31 OCT 83 PHM-TR-84-03

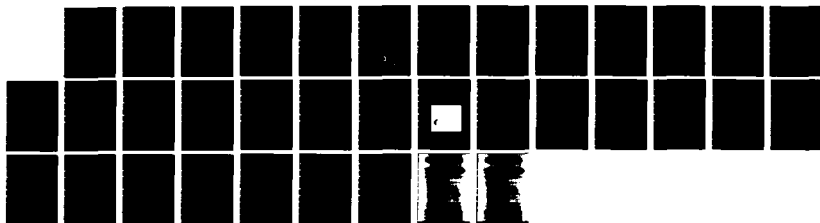
1/1

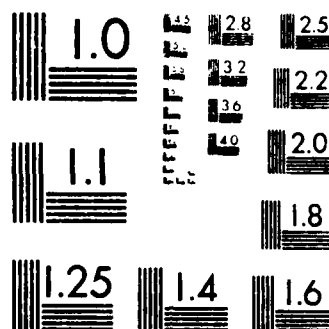
UNCLASSIFIED

AFGL-TR-84-0087 F19628-82-C-0087

F/G 4/1

NL





MICROCOPY RESOLUTION TEST CHART
NATIONAL BUREAU OF STANDARDS 1963-A

12

AFGL-TR-84-0087

TURBULENT DIFFUSION, DISSIPATION, AND WINDS FROM
CALIBRATED PHOTOGRAPHS OF ARTIFICIAL CLOUDS

Christian A. Trowbridge
PhotoMetrics, Inc.
4 Arrow Drive
Woburn, MA 01801

31 October 1983

Final Report for Period 16 April 1982 to 30 September 1983

Approved for public release; distribution unlimited

PREPARED FOR

AIR FORCE GEOPHYSICS LABORATORY
AIR FORCE SYSTEMS COMMAND
UNITED STATES AIR FORCE
HANSCOM AFB, MASSACHUSETTS 01731

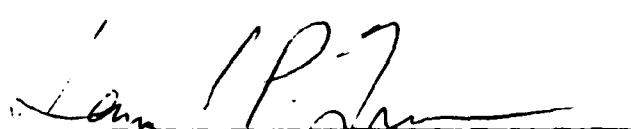
AD-A143 231


DTIC FILE COPY

04 02


This report has been reviewed by the ESD Public Affairs Office (PA) and is releasable to the National Technical Information Service (NTIS).

This technical report has been reviewed and is approved for publication


SAMUEL P. ZIMMERMAN
Contract Manager


DONALD D. GRANTHAM
Branch Chief

FOR THE COMMANDER


ROBERT A. MCCLATCHEY
Director,

Qualified requestors may obtain additional copies from the Defense Technical Information Center. All others should apply to the National Technical Information Service.

If your address has changed, or if you wish to be removed from the mailing list, or if the addressee is no longer employed by your organization, please notify AFGL/DAA, Hanscom AFB, MA. 01731. This will assist us in maintaining a current mailing list.

Do not return copies of this report unless contractual obligations or notices on a specific document requires that it be returned.

SECURITY CLASSIFICATION OF THIS PAGE (When Data Entered)

DD FORM 1473 EDITION OF 1 NOV 65 IS OBSOLETE

50 (14) *Journal of the American Statistical Association*, 1999, Vol. 94, No. 448, Pp. 1029-1039

UNCLASSIFIED

SECURITY CLASSIFICATION OF THIS PAGE (When Data Entered)

20. Abstract (continued)

upper atmosphere turbulence. Turbulent release altitudes were determined by photogrammetric triangulation and by an inverse triangulation method using previously determined wind profiles. Examination of the long term variation of turbopause height suggests that the altitude of the turbopause is a function of the 10.7 cm solar flux.

UNCLASSIFIED

SECURITY CLASSIFICATION OF THIS PAGE (When Data Entered)

FOREWORD

The program described here consisted of quantitative characterization of turbulence present in 90 to 120 km altitude region of the atmosphere. This has been accomplished through computer analysis of photometrically and photogrammetrically calibrated images of chemical tracer releases to determine Fourier turbulence spectra, configuration space statistical descriptors of turbulence and atmospheric winds. Data acquired by in situ measurement techniques (temperature and wind) were often used to supplement information derived photographically. Similar earlier work performed by the PhotoMetrics research group is described in References 1-4, and References 5-10 are examples of the application of the chemical and smoke trail methods to measurement of atmospheric turbulence and dynamics.

The author wishes to express his thanks to Mr. Samuel P. Zimmerman (Technical Monitor) of AFGL for his continued encouragement and support and to K. McDevitt and C. Rice for their contributions to this report.

DTIC
ELECTE
S JUL 20 1984 **D**
B

Accession For	
DTIC	<input checked="" type="checkbox"/>
DTIC	<input type="checkbox"/>
DTIC	<input type="checkbox"/>
By	
Distribution	
Availability Codes	
Dist	Avail and/or Special
A-1	

TABLE OF CONTENTS

Section		Page
	Foreword	3
1	Introduction and Summary	5
2	Eddy Diffusion and Heating Rates	7
	Background	7
	Analysis Method	8
	Determining Further Dynamics	9
	Analysis by Video Densitometry	12
3	Photographic Triangulation	14
4	Turbopause Height Analysis	19
5	Conclusions	28
References	30

List of Illustrations

Figure		
1.	Example of overlay of altitudes found by inverse triangulation	18
2.	Turbopause height data for summer grouping ..	21
3.	Turbopause height data for winter grouping ..	22
4.	Turbopause height as a function of F _{10.7} , summer	24
5.	Turbopause height as a function of F _{10.7} , winter	25
6.	Latitude corrected summer turbopuase height as a function of smoothed 10.7 cm flux	26
7.	Latitude corrected winter turbopause height as a function of smoothed 10.7 cm flux	27

SECTION I

INTRODUCTION AND SUMMARY

The work reported here was directed toward the extraction of turbulent diffusion coefficients and heating rates from photometrically calibrated photographs of chemical smoke tracers released into the atmosphere. Previously reduced data related to turbulent diffusion and transport were also evaluated; specifically atmospheric wind profiles determined by photogrammetric triangulation and temperature and wind profiles measured by falling spheres. Further effort was devoted to an analysis of the long term variation of turbopause height as a function of the solar 10.7 cm flux.

The surface brightness and transport of the chemical tracer clouds are derived by microdensitometrically scanning photographically recorded images of their self-radiation and scattering of sunlight. The reduced data are analyzed to determine both Fourier transform and configuration space descriptors of the fluctuating component of the surface brightness as well as characteristic slope or gradient of the mean brightness distribution. These statistics and features of one dimensional spatial energy spectra are further analyzed to determine rates of dissipation and diffusion coefficients as indicated in Section II. Other methods of calculating heating and eddy diffusivity from wind and temperature data are also contained in Section II, as is an evaluation of the possible application of video densitometry to extraction of the density distributions from the photographs. Transport of the tracer material by wind is determined by triangulation (which also determines the film plate scale or photogrammetric calibration needed to determine turbulence scales) as outlined in Section

III. Also described in this Section is an inverse triangulation method utilized to recover trail altitude and range information from tabulated wind profiles originally determined by triangulation. The task of searching for a long term solar driven variation in turbopause altitude is discussed in Section IV.

SECTION II

EDDY DIFFUSION AND HEATING RATES

Background

Turbulent flow in the atmosphere is initiated and driven by wind shears (Ref 6) and by temperature instabilities produced by differential absorption of solar radiation by different molecular and atomic species. Convective and turbulent transport dominate over simple molecular diffusion through the upper mesosphere and into the lower thermosphere, with the boundary of the turbulent region (the turbopause) varying diurnally and seasonally (and perhaps also over longer periods -- see Section IV) from roughly 90 to 120 km. Computer codes (such as Ref 18) that model atmospheric chemical species concentration profiles take into account this enhanced mixing and transport of species (that is, photochemical generation at one altitude and transport to another (Ref 19)). Additionally, eddy diffusion may affect the absolute atmospheric density and significantly affect vertical heat transport.

Characterization of this turbulent flow may be accomplished by analyzing surface brightness distributions of chemiluminescent or sunlight scattering tracers released from rockets. Fourier and configuration space statistical and numerical analysis methods are applied to these surface brightness distributions to extract information about the turbulent structure. A brief description of the methods and assumptions utilized is presented here (analysis details may be found in references 1-4).

The tracer material released from the rocket (atoms, molecules, or particulates) very quickly reaches pressure and temperature equilibrium with ambient species and is found from experience to conform to the flow field. It is assumed

that local fluctuations in atmospheric particle concentration are traced by means of this sunlight scattering gas or smoke. The spatial characteristics of the flow are frozen in time by radiometrically and photogrammetrically calibrated photography from ground stations at accurately known locations. The surface brightness distribution (a measured of line of sight column density of tracer serves as the starting point for the measurements. Note that the tracer must be optically thin to its own scattered radiation for the surface brightness to be a measure of scale size and tracer distribution (usually assumed gaussian) along the line of sight.

Analysis Method

Analysis proceeds with microdensitometer scans across the images of this frozen flow field, which are assumed (by the ergodic hypothesis) statistically equivalent to the time resolved output of a fixed physical sensor as the flow field moves across it. The resulting digital density information is converted to scene brightness through the H&D characteristic of the film, with appropriate corrections applied to account for reciprocity effects in exposure duration, spectral sensitivity of the film, lens T-stop, and varying sky background (Ref 4). Practical difficulties encountered include film grain noise limitations on spatial sampling which sets the upper wavenumber cutoff for subsequent Fourier analysis; the finite time required to expose a measurable image of the moving cloud causes a smearing of the image which again sets an upper spectral limit; and the limited spatial extent of the cloud sets an analogous cutoff at low wavenumbers and also results in losses in statistical accuracy.

Further corrections are also performed to account for the transfer function of the microdensitometer's finite sampling aperture and for the modulation transfer function of the micro-

densitometer itself, which is a function of the temporal scanning rate of the instrument. To obtain the precision and accuracy needed for these analyses, the response of the data-accessing instrument must be temporally and spatially stationary; for this purpose true microdensitometer optics is required, as explained in Reference 11. (Serious distortion of the calculated power spectra can result from nonuniform reproduction of the photographically recorded data.)

Photogrammetric calibration of the images is also required (as described in Section III) to determine the altitudes of the points of measurement and to convert film plane measurements to distance scales at the glow volume. The sequential analyses often require a correction of scale factor due to the range variation produced by cloud movement in the mean wind field. Finally, the corrected brightness data are analyzed by Fourier (or other statistical) methods. Fourier analysis, or calculation of one dimensional turbulent energy spectra is carried out by one of three methods -- standard Fourier analysis, "fast" Fourier Transform (FFT), or a simple summation process (counting method, Ref 9) which determines the spectral energy in discrete, nonuniform wavenumber bands. Each of these methods requires large amounts of input data to achieve the desired statistical accuracy, usually 20 to 50 parallel microdensitometer scans through the turbulent region of interest. Depending upon analysis method, the average energy spectrum is obtained by segmental averaging or by averaging of spectra derived from individual scans.

Determining Further Dynamics

The one dimensional scalar energy spectrum $E(k)$ as a function of wavenumber k may be utilized to determine the Fourier characteristics of turbulent flow. $E(k)$ often

exhibits power law dependencies on wavenumber, the most well known being the Kolmogoroff or inertial spectral range which implies, from dimensional arguments, that turbulent energy is being fed at a constant rate from large cells into small ones in the subrange of cell dimensions in which this slope obtains. A further application of the energy spectrum is its capability of isolating features of characteristic wavelength -- for example internal atmospheric gravity waves.

When an inertial spectral range is present the heating rate or rate of viscous dissipation of turbulent kinetic energy ϵ may be found as in Ref 1. Further analysis may be performed to determine the kinematic viscosity ν , an eddy diffusion coefficient K , and the Brunt Vaisalia frequency N^2 .

Considerable attention was given to the persistent problem of accurate calculation of the gradient of the mean density structure $\partial n / \partial z$, where n is the mean density and z is altitude. The value of $\partial n / \partial z$ may be used along with the Fourier turbulence spectrum to obtain an estimate of the local heating rate from $E_n(k) = \alpha(n/g) (\partial n / \partial z) \epsilon^{2/3} k^{-5/3}$ where g is gravitational constant, k is wavenumber, and α is a constant. Automatic calculation of $\partial n / \partial z$ from digital microdensitometer recordings of image film density structure have consistently overestimated the gradient of the mean when compared to manual calculation of the gradient from two dimensional microdensitometer recordings. These efforts were aimed at developing an algorithm which would not overestimate the value of the gradient of the mean by typically factors of 20 to 100.

The gradient may be manually determined by calculating the slope $(\partial n / \partial z)$ of the brightness distribution (usually roughly gaussian) transverse to the trail axis. Measurements of contour position taken from the two dimensional microdensitometer

plots of image density are plotted against corresponding brightness data and the slope calculated at the points where the surface brightness has fallen to $1/e^{\text{th}}$ of the maximum brightness. The microdensitometer scanning aperture used to produce these contour plots is large (usually 100-200 μm) and the resulting plots are relatively immune to effects of film grain noise and small scale turbulence structure in the image.

The automatic method uses digital microdensitometer data primarily recorded for use in determining Fourier spectra of turbulence where a small ($\sim 25\mu\text{m}$) scanning aperture is essential to allow calculation of the spectrum at high wavenumbers as well as to prevent aliasing or "folding" of energy from higher to lower wavenumbers. Thus small scale turbulent structure as well as some grain noise is included in this data. Various methods of filtering or smoothing the digital data prior to calculation of the gradient were tested. Simple as well as more complex differentiators were also tried for the actual calculation of the $\partial n/\partial z$. Comparisons to manual calculations performed from equidensity contour plots were disappointing, as none of the automatic methods could consistently provide a slope which compared to better than a factor of 10. The use of longer digital filters provided the best results, however filter length needed to be several times the effective aperture smoothing length used for the equidensity plots. That is, filter length needed to be on the order of one to two millimeters to produce best results, which is a significant fraction of the total scan length for these transverse scans. When parallel scans of digital data were examined significant differences (factors of 3 to 5) in the gradient were noted from scan to scan. By averaging gradients for up to 50 parallel digital scans automatic and manual reduction

methods now generally agree within acceptable factors of 2 to 3. Differences may now be attributed to incomplete smoothing of quantizing "noise" in the digital data and to subjective smoothing applied when measuring positions of contours on the equidensity plots.

Analysis by Video Densitometry

Although as mentioned earlier, true microdensitometer optics is required to obtain sufficient accuracy for Fourier analysis for turbulence, the slow data acquisition rate of the system used led to an investigation of the possible use of an existing computerized video based densitometer. The spatial sampling characteristics (i.e. sampling increment uniformity) of the system were found to be adequate for this task. However the spatial variation of density response for this full field illumination instrument showed both correctable and apparently uncorrectable aberrations in its measurement capability.

Vignetting (shading) due to the densitometer camera lens, nonuniformity of the illumination source, and also the nonuniformity of response over the video photocathode are all correctable. In fact, a single correction step (pixel by pixel) using a previously recorded reference field is all that is needed to effect this time-stationary correction. The reference field is simply the image generated by the video system with no film in its field of view.

The virtually-uncorrectable problem, which is the usual difficulty associated with full field illumination -- the contribution of scattered light -- is that the density response of the system at each pixel is highly dependent upon the micro-density (or light absorption) of the surrounding pixels. It is conceivable that for structurally very simple backgrounds and objects a correction for this flare light

background could be determined. However images of turbulence are certainly not in this category and it is unlikely that suitable algorithms for correction could be developed. New camera sensor techniques are not expected to eliminate this problem. (It remained when a CCD array camera was substituted for the vidicon). Even a linear detector array, which mechanically scans in one direction, would be susceptible to the flare light effect. Flare is controlled in a true microdensitometer by use of narrow field illumination, and a preslit to further limit the illuminated image area to only that micro-area viewed by the narrow field objective lens.

A further nonuniformity, which involved temporal non-stationarity of density response to individual images, was noted. The measured optical density would vary cyclically, apparently in response to changes in ambient room temperature. Although relatively severe (30-40% variation at times), this could be corrected by stabilizing the room temperature.

While most of the problems associated with the use of video based microdensitometry can be adequately corrected, flare effects due to the combination of full field illumination, scattering within the sample, and acceptance angle of the sensor are apparently uncorrectable. Although such systems provide extremely rapid digitization of photographically recorded data the spatial non stationarity of photometric response is considered unacceptable.

SECTION III

PHOTOGRAPHIC TRIANGULATION

Determination of turbulence parameters from photographic records of atmospheric tracer releases requires an accurate knowledge of the true scale sizes at the glow. This is usually accomplished by performing photogrammetric triangulation from two or more photographic projections to determine its three-dimensional spatial location, and hence its range from the camera which defines the conversion from image scale to dimensions at the object. The methods used to perform these scale calibrations are detailed in References 12 and 13, with further information on their applications in References 14 and 15. A brief description of the technique is presented here.

Photographic triangulation to distant objects is based upon accurate knowledge of the location and orientation of each camera photographing the object. The location is usually expressed in latitude, longitude, and altitude (referenced to an earth ellipsoid model), which are determined by surveying the camera positions. Positions may sometimes be scaled from USGS topographic maps, although the lower accuracy may severely degrade the triangulation results. The orientation of the camera (the angles which describe the viewing direction) is determined by analysis of images which have recorded the star field at accurately known times. The film frames with star images are semiautomatically aligned on the film digitizer (Ref 14) such that an orthogonal coordinate system defined by the film fiducial markers (coordinate (0,0) is the camera optic axis) coincides with the digitizer axes. A digital star catalog is searched to determine which stars are in the field

of view and the digitizer semiautomatically locates each star image and records its film plane coordinates along with equatorial coordinates (right ascension and declination) of the star corrected to the precise time of the exposure. The film plane and equatorial coordinates for up to 20 stars are related through vector equations which are solved to determine the lens focal length (using star triplets) and also the direction in space of the camera optic axis (using pairs of stars). The orientation of the optic axis is calculated in right ascension and declination, and also an angular rotation needed to bring the star and image locations into coincidence. It is often more convenient either for ease of visualization or for further calculation, to express (the orientation in some other coordinate system (such a horizon or geocentric); this is easily accomplished through coordinate transformation of the optic axis line of sight vector (rotations about coordinate axes).

Time-coincident frames from two photographic observation sites are digitized using the same automatic scanning densitometer as used for star frames. This system locates and digitizes the film plane coordinates of the centerline of the glow image for use by the triangulation routines. Turbulent regions of releases often do not have readily identifiable centerlines and automatic reduction of the film density distribution transverse to the trail axis to locate the center is ineffective. They may however have "blobs" of tracer material which are uniquely identifiable from each site whose coordinates may be digitized. Further, when only approximate altitude information is needed (to associate altitudes with energy spectra or other turbulence parameters) a series of small "dots" or marks may be subjectively placed on each film (or an overlay) along the trail "centerline."

While positions of these dots are easily digitized, the resulting triangulation is imprecise (dots on one image will generally not correspond closely to dots on the other triangulation image) and interpolation is required to associate space positions with each dot location.

The digital film plane positions define a series of vectors to the tracer glow from each photographic site and are used to define the spatial location of the glow. An iterative procedure is used to determine the best match of each site 1 line-of-sight vector with a line-of-sight vector from site 2. The point of intersection (or closest approach) of each vector pair is found in the geocentric coordinate system, converted to latitude, longitude, altitude in the geographic system, and tabulated for association with a particular point on each film image. Although conceptually the technique for triangulation is straightforward there are problems associated with the implementation of the method, some of which are detailed in Ref 15. These problems are primarily with the design of the iterative routines which determine the "best match" pairing of points using a dihedral angular matching criterion and with resolving trail segments which lie nearly along a uniform line of sight when viewed from one of the photographic projections.

Triangulation is also the first step in remote measurement of the wind field at high altitudes. The trail position is first determined for several photographic frame pairs extending over total durations of one to two minutes. Each altitude profile of position is spline interpolated to a convenient equal altitude grid and least square analysis of trail position as a function of time is applied to each altitude to yield average positional changes, average velocity components, and their associated errors.

An inversion of the triangulation method has been used as a reconstruction technique to allow identification of altitudes on films of previously-made releases for which much of the supporting information has been lost or discarded, or for which only one of the original triangulation films is available. These chemical releases had been used primarily to determine molecular diffusion coefficients and wind field (using overlays with manually placed dots). When the overlays or the computer printout of dot number and its triangulated altitude are missing it is still possible to use the profile of wind components (which are available in the analyzed data reported) to assign altitudes along the trail image.

Utilizing the known trajectory of the release rocket and the known camera parameters (focal length, azimuth, elevation, altitude, latitude and longitude) a computer program first constructs a model release along the trajectory. This line release is then transported using the known wind profile and at predetermined increments of time (matched to the photographic times) vector triangulation determines the projection of the release into the film plane of the particular camera. Computer generated plots of the image plane at 1 km altitude intervals were then used as overlays to establish an altitude grid on the release film (Fig 1). The major sources of error in this inverse triangulation arise from uncertainty in site locations and the generally few points on the trajectory which are known (often these points used are not actually on the trajectory). Estimated altitude errors have been in the 1-4 km range when using this method.

FRAME TIME= 240.00

ALT	LAT	LON	VE	VN	RANGE	N
98.00	30.131	86.579	73.0	-21.0	169.78	1
99.00	30.097	86.556	85.0	-32.0	173.31	2
100.00	30.050	86.562	83.0	-49.0	178.25	3
101.00	30.042	86.607	61.0	-49.0	179.80	4
102.00	30.064	86.680	24.0	-36.0	179.08	5
103.00	30.094	86.737	-5.0	-19.0	177.58	6
104.00	30.123	86.744	-9.0	-2.0	175.80	7
105.00	30.144	86.742	-8.0	12.0	174.48	8
106.00	30.148	86.733	-3.0	18.0	174.64	9
107.00	30.134	86.707	11.0	16.0	176.13	10
108.00	30.088	86.683	24.0	-1.0	180.49	11



Figure 1. Example of overlay of altitudes found by inverse triangulation for release Paula Oct 1962 (Eglin Air Force Base site M).

SECTION IV

TURBOPAUSE HEIGHT ANALYSIS

Analyses were performed in an effort to characterize the height of the turbopause as a function of several geophysical variables. The principal purpose of this analysis was to investigate long term (~16 years) variation of turbopause height (Z_T) as a function of the 10.7 cm radiation from the sun ($F_{10.7}$), and the planetary magnetic disturbance indices K_p and A_p . It has been suggested (Ref 16) that there is a strong solar cycle variability of Z_T associated with long term changes in the 10.7 cm flux and possibly also associated with the K_p and A_p indices, which themselves also correlate with the 11 year solar cycle.

The data base used for analysis is comprised of measurements of turbopause height determined from AFGL chemical release programs conducted at Eglin Air Force Base from 1962 to 1976 and from heights deducted from Ar/N₂ ratios measured by rocketborne mass spectrometers at Heiss Island from 1968 to 1977. Associated with each Z_T is the $F_{10.7}$ flux, K_p and A_p indices.

The most desirable method of analysis for extraction of dependencies of Z_T on many variables is multivariate regression analysis. Such an analysis would determine how well (in terms of regression coefficients and standard deviations) the measured data corresponds to hypothesized functional forms for the variation of each independent parameter. This was not employed because of the limited number of measurements relative to the number of variables. Confidence in the results would be greatly diminished because of large standard deviations.

Our approach to determining any long term variations was to attempt to remove the sources of short term variation (semi diurnal, diurnal, seasonal) from the data and then examine the remaining trends, if any. The data were hence divided into winter and summer groupings (16 Sept to 15 Mar and 16 Mar to 15 Sept respectively) similar to References 16 and 17, and an approximate form for the diurnal variation used to modify the observed Z values such that all would be representative of the height at a uniform local time (0600 for winter, 0300 for summer). Each of these times correspond to an altitude of 105 km. The forms for diurnal variation were semiquantitatively chosen since the majority of the data is clustered near 0300 hours and 2000 hours. The preponderance of measurements near twilight results from conditions necessary to photograph high altitude sunlight scattering releases; good contrast may only be obtained when the observation camera is in darkness while the tracer material is still sunlit. Some of the releases were chemi or self luminescent allowing nighttime measurements to be performed. Semi diurnal corrections were not attempted due to this clustered nature of the measurements. Furthermore, after diurnal corrections were applied to the seasonally separated Z_T values, multiple measurements performed within the same year had their Z_T and $F_{10.7}$ values averaged.

Figures 2 and 3 show the variation of Z_T as a function of local time for the summer and winter groups respectively. Each figure also shows the diurnal form which was used for correction purposes. It is, of course possible that some of the apparent diurnal change could due to long term effects associated with the limited number of samples. The nighttime rise of the turbopause is, however, clearly demonstrated by the series of chemical release measurements (dashed line-winter) made on a single night and hence only the specific form of the diurnal variation may be questioned.

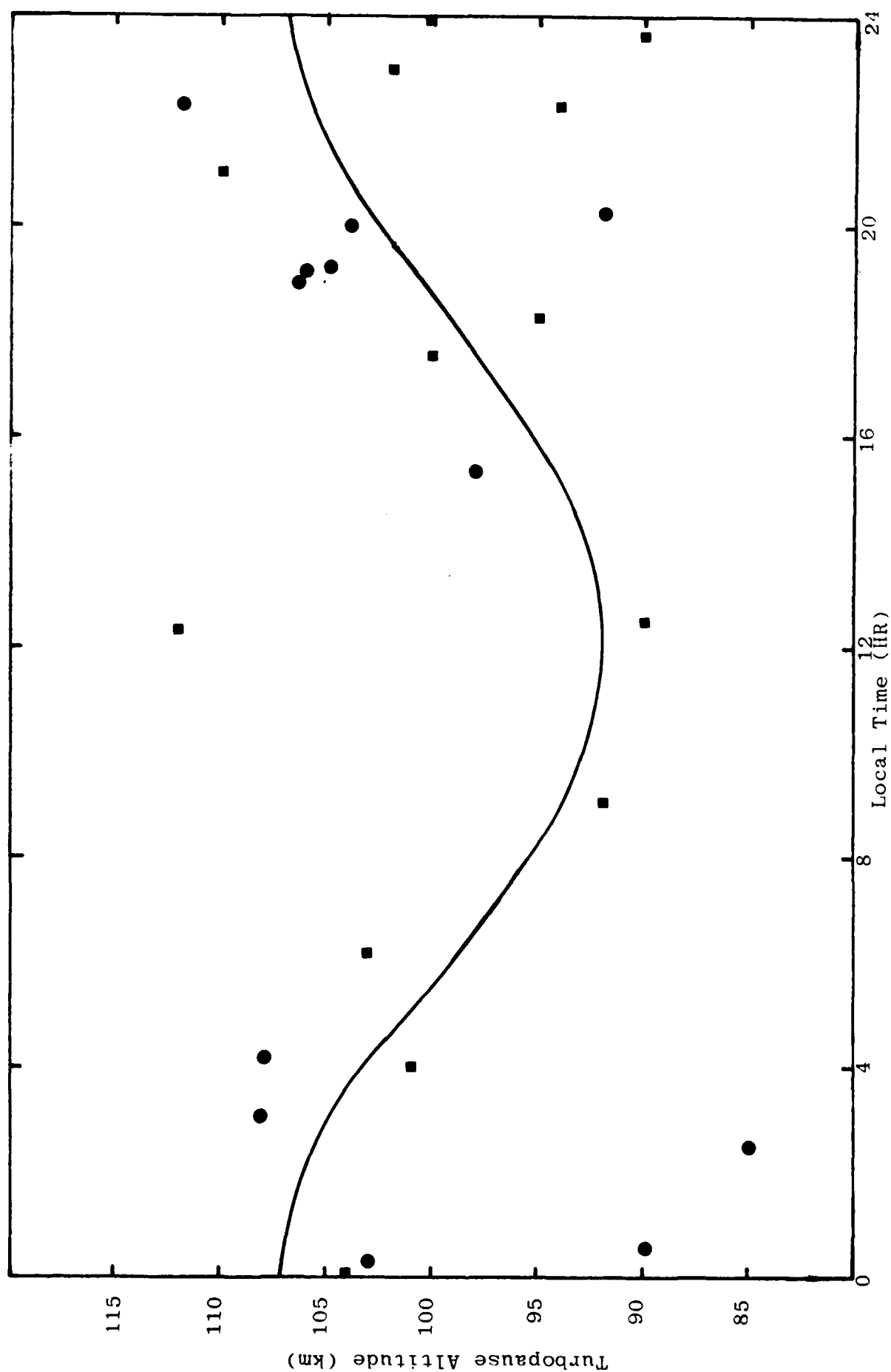


Figure 2. Turbopause height data for the summer grouping with diurnal variation curve estimated. Dots represent data measured at Eglin AFB and squares at Heiss Island.

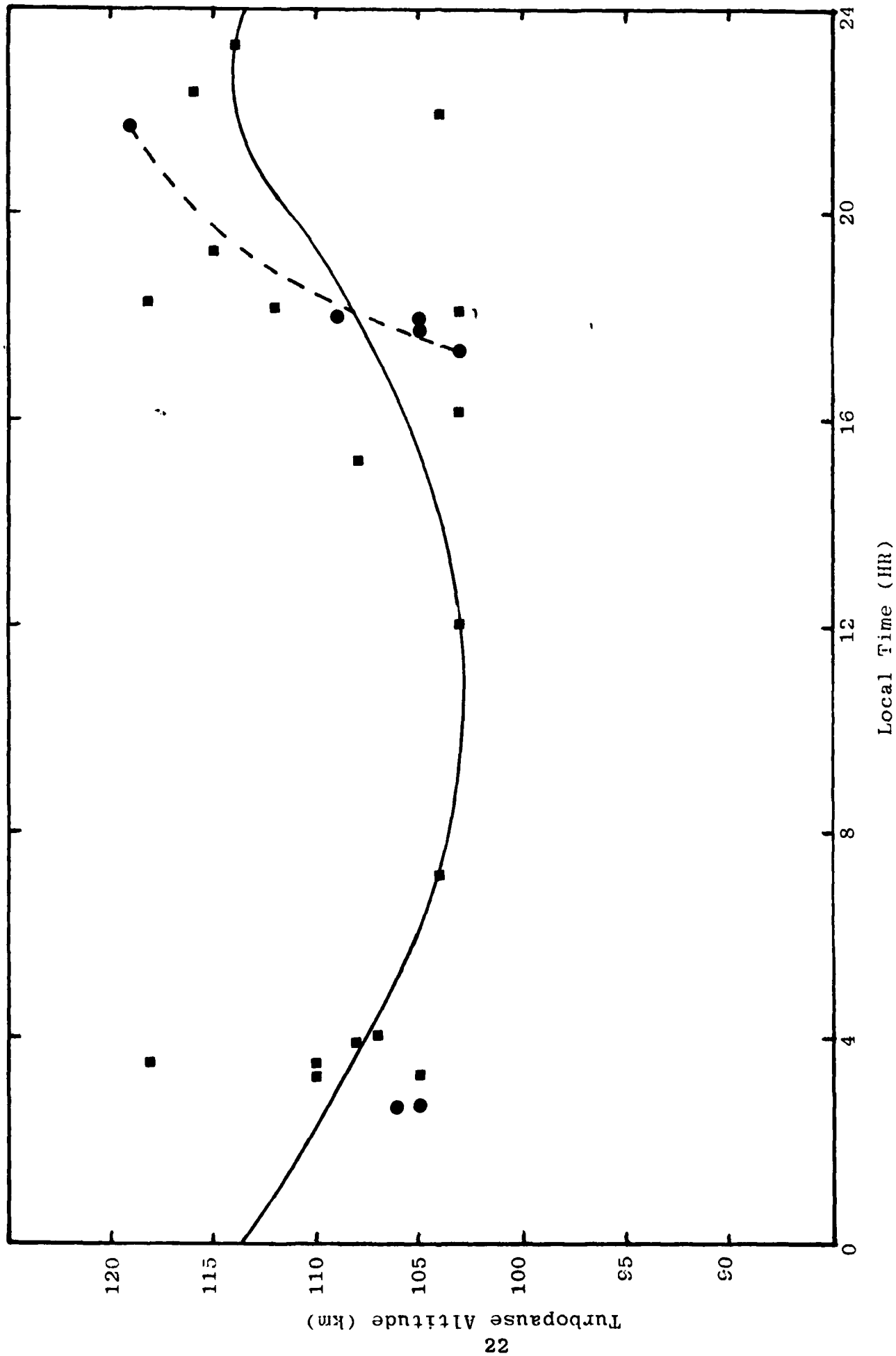


Figure 3. Turbopause height data for the winter grouping with diurnal variation curve estimated. Dashed curve shows the nighttime rise determined from experiments performed on one night (1962). Dots represent data measured at Eglin AFB

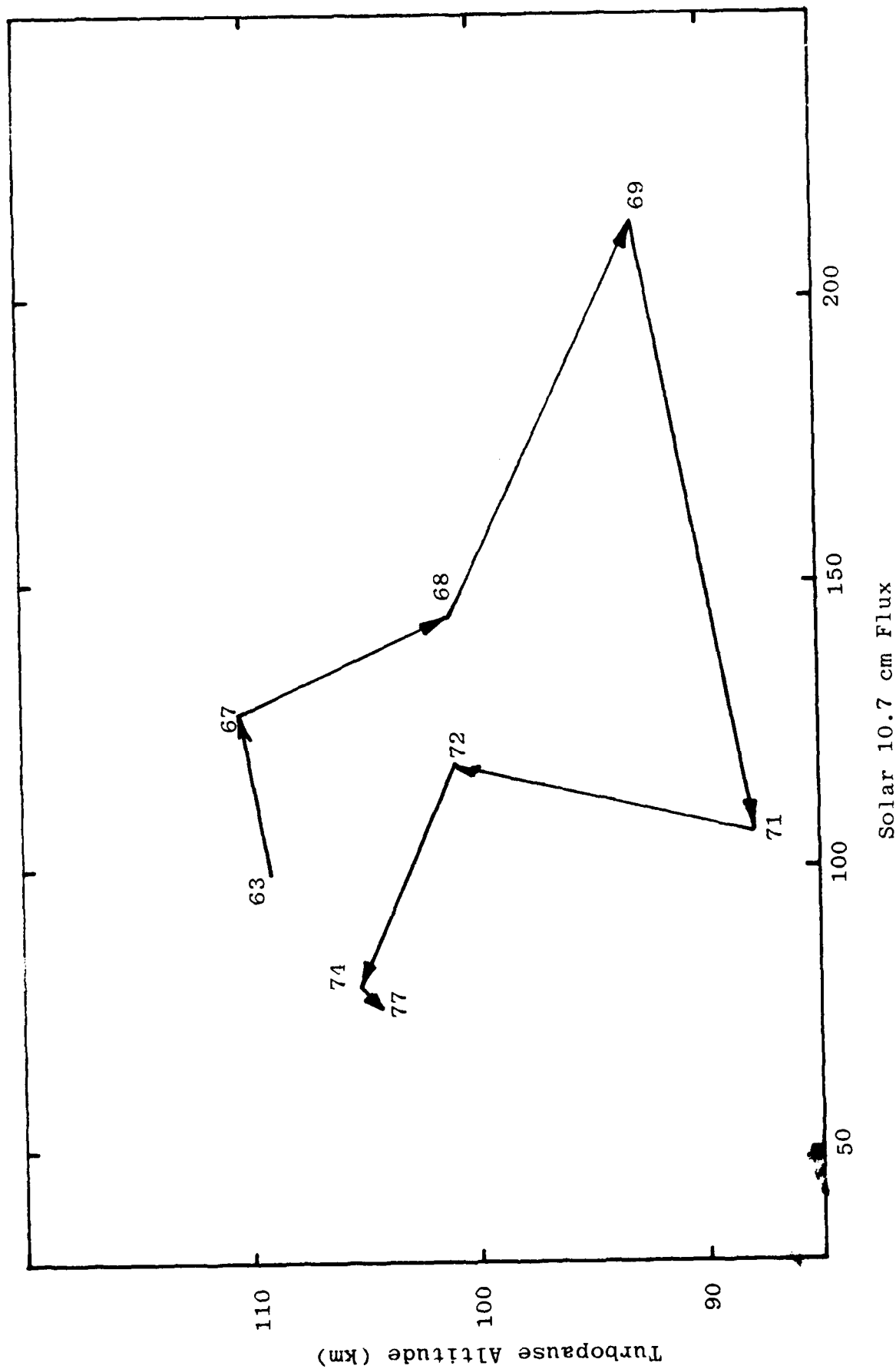


Figure 4. Turbopause height as a function of $F_{10.7}$, summer. Data have been corrected for diurnal variation and averaged by year.

The behavior of seasonal turbopause height by year as a function of $F_{10.7}$ is shown in Figures 4 and 5. These data have been corrected for diurnal variation and Z_T and flux values averaged by year. These data with year associated with each measurement appear to show a hysteresis or lagging of the altitude response to changes in the decimeter flux. This is most clearly demonstrated by the clockwise circulation in the summer data; winter data appear to circulate counter-clockwise.

Results of further attempts to remove uncertainty due to latitude and possible short term changes in flux are shown in Figures 6 and 7. An obvious systematic altitude differential between the 30°N and 80°N data was compensated by estimating the average altitude shift needed to make the diurnal variation curves representative of either the 30°N or 80°N data. Furthermore it was assumed that altitude changes in response to changes in $F_{10.7}$ do not occur rapidly and a smoothed average flux was substituted for the yearly seasonal averages. Note that the direction of circulation is now approximately clockwise for both summer and winter data. The standard deviations of the mean altitude are 2.5 km and 7 km for winter and summer respectively. Both sets of data have excursions barely exceeding ± 1 sigma, and while they may be suggestive of a long term dependence upon $F_{10.7}$, they also may be considered as samples of a normal distribution of altitudes (t test at 95% confidence). Further analysis could be conducted using this data, especially the inclusion of the K_p and A_p values which presumably could reinforce the result by demonstrating similar Z_T dependence upon other solar derived parameters.

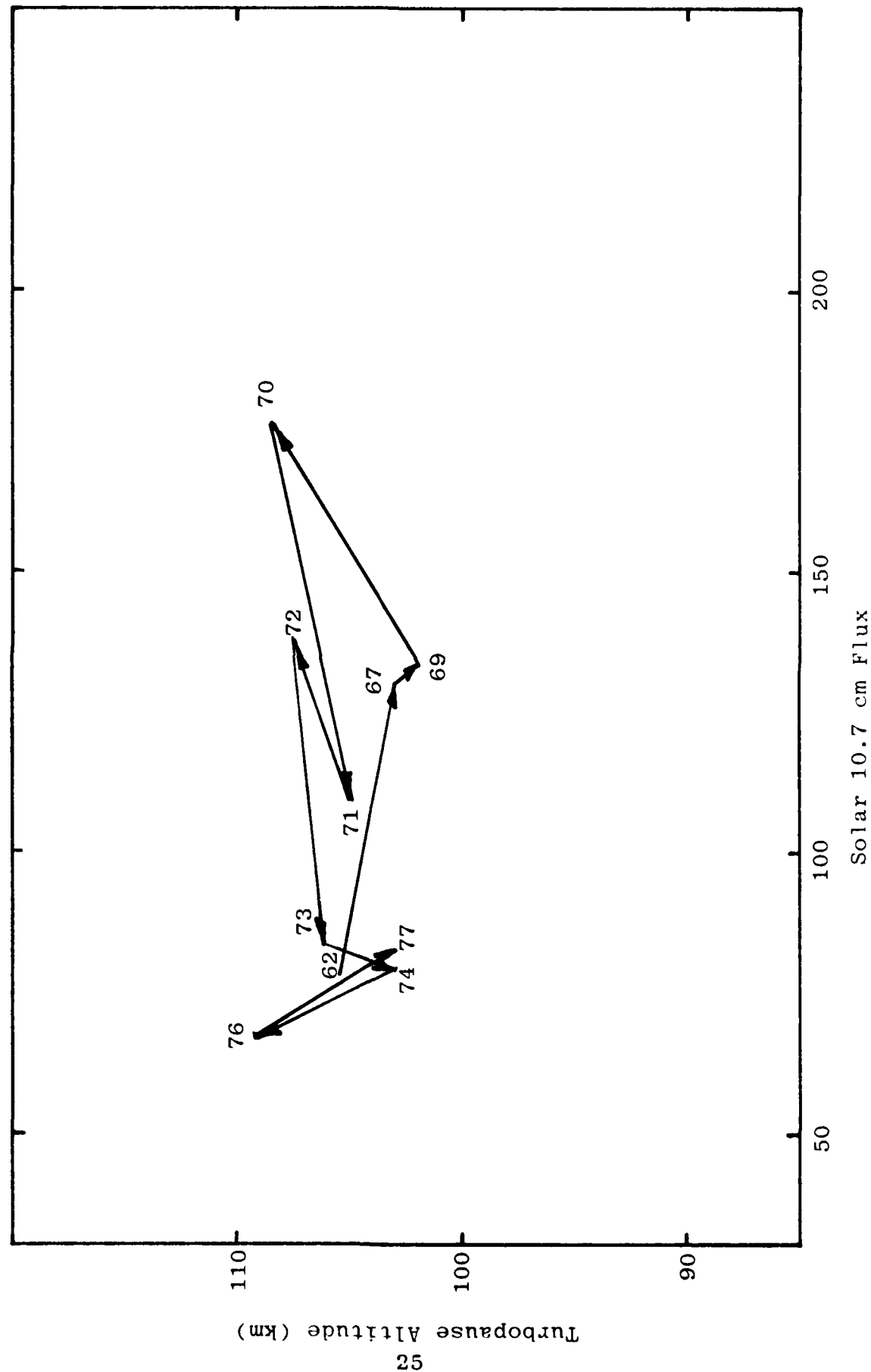


Figure 5. Turbopause height as a function of $F_{10.7}$, winter. Data have been corrected for diurnal variation and averaged by year.

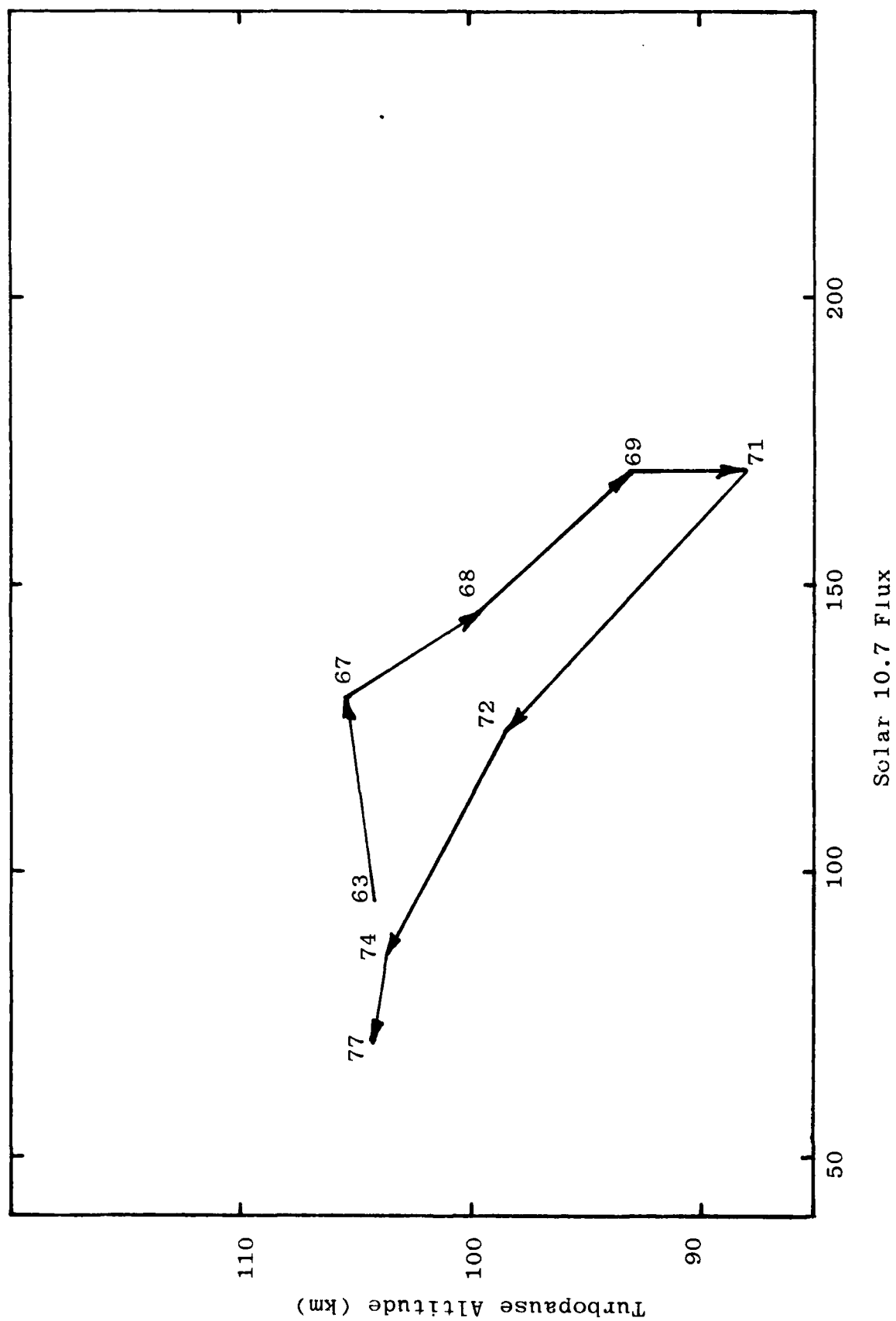


Figure 6. Summer turbopause height corrected for observation latitude as a function of smoothed 10.7 cm solar flux.

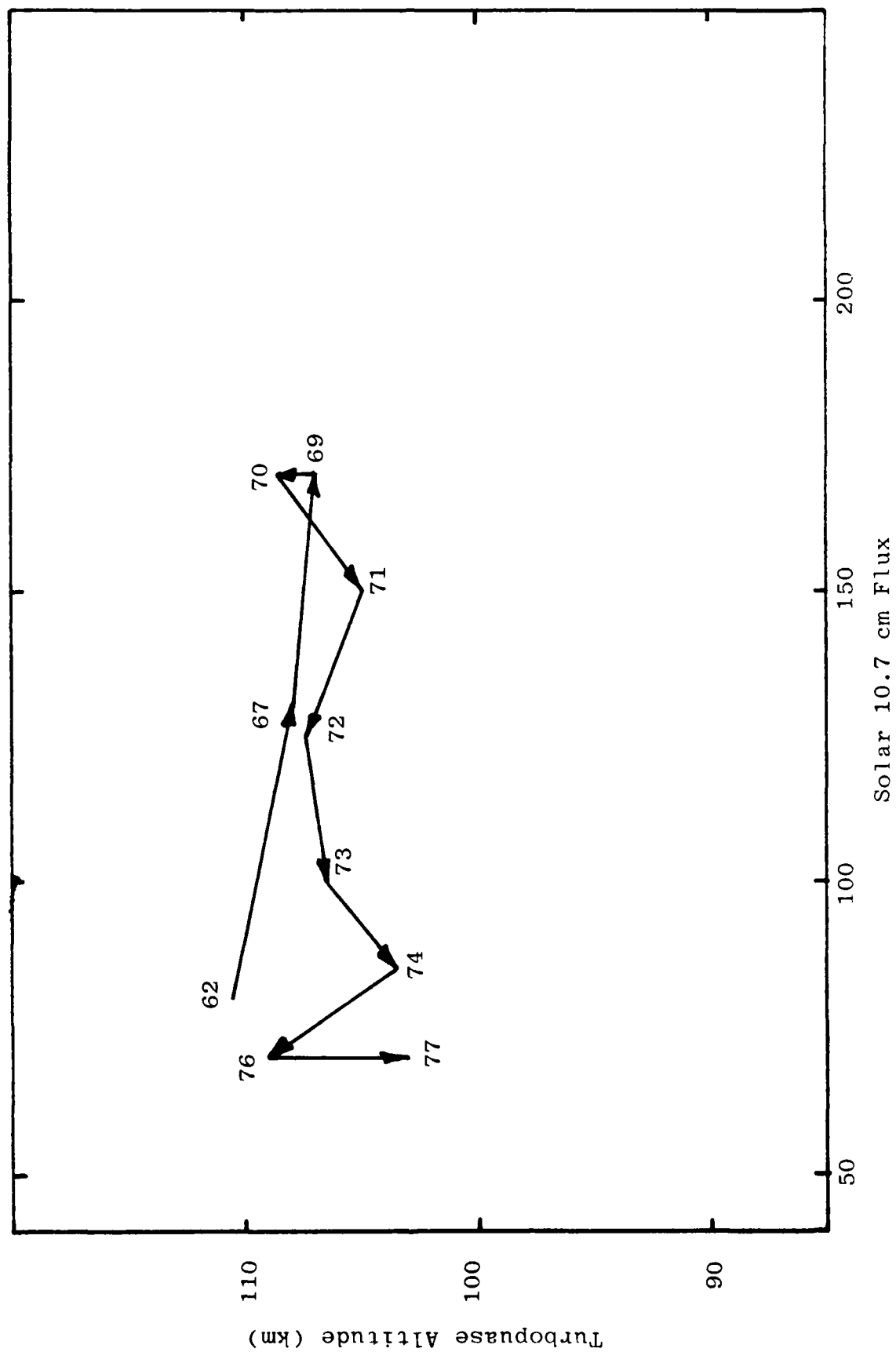


Figure 7. Winter turbopause height corrected for observation latitude as a function of smoothed 10.7 cm solar flux.

SECTION V

CONCLUSIONS

Techniques developed and refined over the past several years have been applied to extract and analyze data from photographic records of chemical releases to provide turbulent diffusion and dissipation in the region of the turbopause. Fourier turbulence spectra, the gradient of mean density distribution $\partial n / \partial z$, the rate of change of turbulent density fluctuations, and horizontal wind and shears were utilized to determine diffusion and heating.

Since the gradient of the mean brightness distribution when combined with numerical parameters of the energy spectra has provided the most reliable measurements of these quantities, methods to refine the calculation of gradient were investigated. Several techniques were applied to the tasks of automatically computing the gradient from the digital photographic records, none of which would consistently yield results strictly comparable to manually derived values. Remaining factors of 2 to 3 difference are probably attributable to insufficient smoothing of quantizing "noise" of the digital data and to subjective smoothing done during manual reduction of the gradients. Two dimensional spatial filtering of the digital data may provide for removal of this "noise," or an interactive approach could be utilized to simulate the manual reduction method.

The search for a more rapid way to extract density information from the photographs led to examination of video access methods. Although video techniques are suitable for some applications which require quantitative measurement of film density, currently available corrections for "crosstalk"

are not adequate to provide suitably accurate turbulence measurements. Primarily, flare light effects due to full field illumination vary with the densities and spatial content of the image, making calibration difficult, if not impossible, as image complexity increases.

Identification of the altitude (as well as establishing the film plate scale) where turbulence measurements were made was done by triangulation when sufficiently accurate records of site locations and other release data were available. Alternatively, a less accurate reconstruction technique (inverse triangulation) was employed when adequate calibration data were not available.

Analysis was performed to establish a probable long term relationship between turbopause height and solar 10.7 centimeter flux. The results suggest a lagging 11 year cycle of motion of the turbopause altitude in response to the F_{10.7} flux. Confidence in the results is not great because of the limited data available. Analysis of the corresponding K_p and A_p magnetic index data could possibly establish a similar solar activity altitude dependence.

The results of the data analysis for turbulence parameters were reported to AFGL scientists as they were obtained, and are on file at the LYT Branch of AFGL.

REFERENCES

1. C.A. Trowbridge, Determination of Upper Atmospheric Winds and Turbulent Diffusion and Dissipation from Artificial Cloud Expansion and Growth, AFGL-TR-81-0200, 22 Jul 1981, AD A106387.
2. C.A. Trowbridge, and I.L. Kofsky, Densitometric Analysis to Determine Artificial Cloud Expansion Characteristics, AFCRL-TR-75-0147, 14 Mar 75, AD A013777.
3. C.A. Trowbridge, Densitometric Analyses to Determine Artificial Cloud Expansion Characteristics, AFGL-TR-78-0075, 15 Mar 1978.
4. I.L. Kofsky, C.A. Trowbridge, and R.H. Johnson, Analysis of Chemical and Smoke Releases in the Atmosphere, AFCRL-TR-74-0102, 31 Jan 1974, AD 783909.
5. S.P. Zimmerman, N.W. Rosenberg, A.C. Faire, D. Golomb, E.A. Murphy, W.K. Vickery, C.A. Trowbridge, and D. Rees, The Aladdin II Experiment: Part 1, Dynamics, Space Research XIV (1974).
6. S.P. Zimmerman, J. Appl. Meteorol. 4, 279 (1965).
7. S.P. Zimmerman, and C.A. Trowbridge, The Measurement of Turbulent Spectra and Diffusion Coefficients in the Altitude Region 95 to ~110 km, Space Research XII (1973).
8. S.P. Zimmerman, and N.V. Loving, Turbulent Dissipation and Diffusivities in the Stratosphere, CIAP-DOT, Volume 1, The Natural Stratosphere (1974).
9. S.P. Zimmerman, Turbulence Observed in Electron Density Fluctuations in the Equatorial E Region over Thumba, India -- A Reanalysis, J. Geophys. Res. 81, 5201 (Oct 1976).
10. S.P. Zimmerman, A.F. Quesada, V.L. Corbin, C.A. Trowbridge, and R. Olsen, Dept of Transportation, CIAP Sponsored Research Final Report.
11. I.L. Kofsky, Reduction of Pictorial Data by Microdensitometry, Chapter in "Aerospace Measurement Techniques," (ed. G.G. Manella), NASA SP-132, January 1967.
12. A.F. Quesada, Vector Evaluation of Triangulation Camera Parameters from Star Photographs, AFCRL-TR-75-0451, 21 Aug 1975, AD A01965.

13. A.F. Quesada, Application of Vector and Matrix Methods to Triangulation of Chemical Releases in the Upper Atmosphere, AFCRL-71-0233, 23 April 1971, AD 729448.
14. C.A. Trowbridge, and W.S. Andrus, An Automated Coordinate Measurement System for Smoke Trail Photographs, AFGL-TR-78-0231, 29 Sept 1978, AD A062485.
15. C.A. Trowbridge, I.L. Kofsky and R.H. Johnson, Recording and Analysis of Optical Data from Stratospheric Dynamics Experiments, AFGL-TR-78-0015, 14 Jan 1978, AD A054013.
16. S.P. Zimmerman and T.J. Keneshea, Solar Cycle and Magnetic Index Relations to Turbopause Height, presented at COSPAR, Toronto 1982.
17. S.P. Zimmerman, The Diurnal Variation of Turbopause Height, AFGL-TR-80-0332, 3 Nov 1980, AD A099340.
18. T.J. Keneshea, S.P. Zimmerman and C.R. Philbrick, A Dynamic Model of the Mesosphere and Lower Thermosphere, Planet. Space Sci., 27, 385 (1979).
19. J.D. George, S.P. Zimmerman, and T.J. Keneshea, The Latitudinal Variation of Major and Minor Neutral Species in the Upper Atmosphere, Space Research XII (1972).

FINED

FILMED

END

FILMED

1974